Power measurement of frequency-locked Smith-Purcell radiation

Amit S. Kesar,* Roark A. Marsh, and Richard J. Temkin

Plasma Science and Fusion Center, Massachusetts Institute of Technology, 167 Albany Street, Cambridge, Massachusetts 02139, USA

(Received 19 October 2005; published 7 February 2006)

Frequency-locked Smith-Purcell radiation (FL-SPR), generated by a train of electron bunches traveling above a grating, is characterized by a broad range of frequencies which are locked to the train frequency in a discrete comb and are spatially dispersed in space. We report absolute-scale power measurement of FL-SPR in the millimeter wave range. A 50 ns long train of 170 μm electron bunches was produced by a 15 MeV, 17 GHz accelerator with 80 mA of average current. The grating had 20 periods spaced by 2.54 mm. The experimental results were compared, on an absolute scale, with the electric-field integral equation model which takes into consideration the finite length of the grating. Very good agreement was obtained. The present results should be useful in planning SPR applications such as diagnostics of electron bunch length on the femtosecond scale and coherent THz radiation sources.

DOI: 10.1103/PhysRevSTAB.9.022801 PACS numbers: 41.60.−m, 52.70.Gw, 02.70.Dh, 42.25.Fx

I. INTRODUCTION

Smith-Purcell radiation (SPR) [1] emitted by an electron bunch passing at a relativistic velocity $\beta = (1 - \gamma^{-2})^{1/2}$ above a periodic structure is characterized by a broad spectrum of frequencies in which the radiated wavelength depends on the observation angle according to the SPR resonance relationship. Though different theoretical models agree on this resonance relationship, substantial differences arise in the calculated radiated energy [2]. An exact energy measurement is important for examining the accuracy of the theoretical models and can lead to a higher accuracy of SPR applications.

For the setup illustrated in Fig. 1, the nth harmonic of the radiated wavelength λ depends on the grating period D_g and the observation angles θ and ϕ by the SPR resonance relationship

$$\lambda = \frac{D_g}{n}\left(\frac{1}{\beta} - \sin\theta \sin\phi\right), \tag{1}$$

and the bandwidth is inversely proportional to the number of grating periods, N_g. The coordinate system is shown in Fig. 1 and is consistent with our previous paper, Ref. [2]. We choose the electron beam to be moving in the x direction. We orient our grating so that the lines of the grating are orthogonal to the beam direction, and we label the direction of the grooves to be the y direction. The wave vector of the radiation, $\mathbf{k}$, makes an angle ϕ with respect to this y axis. The other angle in the spherical coordinate system, θ, is defined as the angle of the projection of the $\mathbf{k}$ vector on the x-z plane. From the definitions of ϕ and θ, it follows that the components of the wave vector are $k_x = k\sin\phi\sin\theta$, $k_y = k\cos\phi$, and $k_z = k\sin\phi\cos\theta$, where $k = \omega/c$ is the wave number and ω is the angular frequency. An auxiliary angle $\phi_b = 90 - \phi$ is sometimes used for convenience with the experimental setup (see Fig. 1).

SPR can be used for beam diagnostics. Coherent radiation is observed at angles which correspond to wavelengths larger than, or on the order of, the bunch length [3]. Thus SPR can be used as a nondestructive bunch-length diagnostic tool by determining the angle of cutoff in coherent radiation [4,5]. Subpicosecond bunch-length measurements were obtained by measuring the angular SPR pattern from 15 MeV bunches [6]. Other diagnostics may include a position sensor for ultrarelativistic beams [7] and an electron bunch shape measurement [8].

Optical SPR wavelengths were observed from an electron beam of 855 MeV [9]. Forward directed partially coherent SPR from relativistic electrons is reported in [10]. Coherent SPR from short electron bunches is reported in [11,12]. Observation of frequency-locked coherent terahertz SPR is reported in [13].

A number of theoretical models are used to describe SPR. An exact model was derived by van den Berg for an infinitely long periodic grating with a line [14] or a point [15] charge passing above it. Based on van den Berg's method, SPR for electrons with energies of 1–100 MeV was calculated by Haeberlé *et al.* [16].

A grating surface current model based on the image-charge approximation was developed by Walsh *et al.* for a strip grating [17] and was generalized by Brownell *et al.* for a grating of arbitrary shape [18]. Optimization of the radiated energy for very high charge energies is described in [19,20] for a strip and a blazed grating, respectively.

The SPR from a line of charge was calculated by two independent models, based on the finite-difference time-domain and the electric-field integral equation (EFIE) methods, respectively [21]. Very good agreement was obtained between these models and it was shown that the finite length of the grating has to be taken into account. The EFIE model has recently been extended to the case of a point charge where it was shown to be consistent with van

*Electronic address: kesar@alum.mit.edu

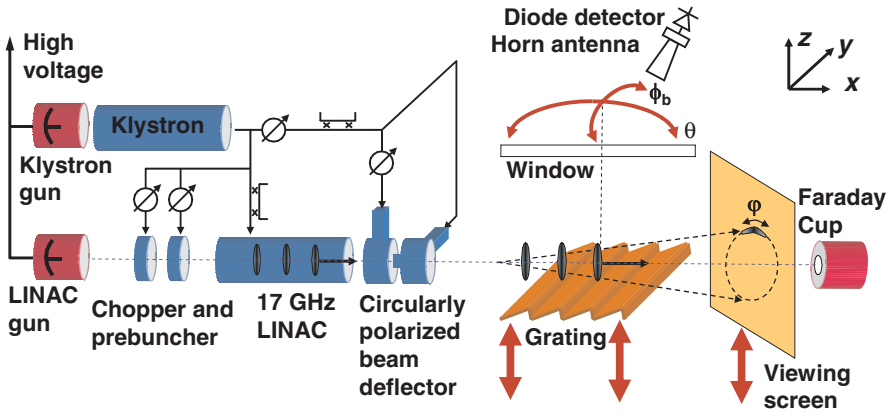

FIG. 1. (Color) SPR experimental setup (not to scale) including the klystron, linac, deflecting cavities and screen, and the grating.

den Berg's model for the special case of an infinitely long grating [2].

Previously, very good agreement was obtained between theoretical predictions and the distribution of SPR energy, on an arbitrary scale, versus the observation angles. These results validate the SPR resonance condition, Eq. (1). However, the absolute-scale comparison of the radiated power vs. angle has previously been limited to an order of magnitude agreement with one of the models, as in [8,10,12,22–25].

In the optical SPR from an 855 MeV electron beam, reported by Kube *et al.* [9], the radiation factor which corresponds to the grating efficiency was extracted from the intensity measurements. This factor was then compared to calculations using van den Berg's model and a surface current model similar to the image-charge approximation. While a fair agreement was obtained with van den Berg's model, the radiation by the surface current model was 6 orders of magnitudes higher. This difference was emphasized by the high beam energy of 855 MeV because the radiation factor by van den Berg's model scales inversely proportional to γ^2 whereas the radiation factor by the image-charge approximation is hardly sensitive to the beam energy. In other SPR experiments, conducted at lower beam energies, accurate comparisons of the radiated power with theory have not been previously reported. Such comparisons are more difficult since the number of grating periods would not be expected to be sufficiently large to use the infinite grating approximation of the van den Berg model, as discussed further in this paper.

The objectives of this paper are to obtain an accurate power measurement on an absolute scale of SPR from a train of 15 MeV electron bunches produced by the 17 GHz linear accelerator (linac) at MIT, and to compare the results to those from the finite grating length EFIE model [2]. This comparison requires slight modification of the EFIE model to the case of a train of bunches, and is described below.

In the finite grating length EFIE model in [2], the radiated energy from a single charge passing above the grating is found by calculating the far-field magnetic component $\mathbf{H}(r, \theta, \phi, \omega)$, where r is the distance between the grating and the observer. Thus, the angular distribution of the nth order radiated energy density, $E_n(\theta, \phi)$, is

$$E_n(\theta, \phi) = (Z_0 r^2/\pi) \int_{0.5\omega_n}^{1.5\omega_n} |\mathbf{H}(r, \theta, \phi, \omega)|^2 d\omega, \quad (2)$$

where $\omega_n = 2\pi nc/D_g(\beta^{-1} - \sin\theta \sin\phi)$.

For a periodic train of bunches at a repetition frequency $f_{RF} = \omega_{RF}/2\pi$, the radiation would be locked to discrete angular frequencies $\omega_m = m\omega_{RF}$ [13]. For our accelerator, the repetition frequency is the same as the accelerator frequency, namely, 17.14 GHz. At these frequencies, the Fourier components of the magnetic field from the train of bunches are $\mathbf{H_m}(r, \theta, \phi) = f_{RF}\mathbf{H}(r, \theta, \phi, \omega_m)$. In this case, the nth order radiated power density (in units of W/sr) is

$$S_n(\theta, \phi) = \frac{Z_0 r^2}{\pi} \sum_m |\mathbf{H_m}(r, \theta, \phi)|^2, \quad (3)$$

where the summation is in the range of frequencies $0.5\omega_n < \omega_m < 1.5\omega_n$.

II. EXERIMENTAL SETUP

The experimental setup is illustrated in Fig. 1. The experimental parameters are described in Table I, unless otherwise specified.

A 15 MeV ($\gamma = 30$), 80 mA train of periodic electron bunches at an rf repetition frequency of 17.140 GHz (each bunch charge is 4.67 pC), was produced by the 17 GHz linac built by Haimson Research Corporation (HRC) [26]. The linac was powered by 10 MW, 17.140 GHz, 110 ns flattop pulses from an HRC relativistic klystron [27]. The linac filling time is 60 ns, thus for each macro pulse, the output train was steady state at 15 MeV for ~50 ns. The electron beam into the linac was produced by a thermionic electron gun, a chopper, prebuncher, and three lenses (not shown in Fig. 1) [28]. The linac and klystron guns were operated at 525 kV, 0.5 Hz, with 1 μs flattop pulses from a high-voltage modulator [29]. A small portion of the klys-

TABLE I. Smith-Purcell experiment parameters

Average current I_b	80 mA
Train relativistic factor γ	30
Train frequency f_{RF}	17.140 GHz
Height above the grating, $b_{\min}$	2 mm
Bunch length σ_x	170 μm
Grating period D_g	2.54 mm
Blaze angle α	30°
Number of periods, N_g	20
Grating width, W	100 mm

tron power was used to drive the chopper and prebuncher at $\sim$1.5 kW each, via variable attenuators and phase shifters. The electron beam full-width at half maximum (FWHM) was $\sim$1 mm in diameter with an emittance of 3π mm mrad. The beam average current, I_b, was measured by a beam monitor located at the accelerator output and by a Faraday Cup located at the end of the beam line.

The length of the bunches in the train could be measured directly with an HRC circularly polarized beam deflector followed by a toroidal focusing lens (not shown in Fig. 1), a 3 m drift section and a viewing screen [30,31]. The deflector consists of vertical and horizontal deflecting arms, and a set of variable power splitters and phase shifters. When a direct measurement was required, about 200 kW of the klystron power was transferred through a high-power hybrid splitter to drive the deflector arms. For these operating parameters the measured FWHM bunch length was $\sigma_x = 170 \pm 30$ μm.

The grating was made from oxygen-free high conductivity copper and was located 2 m downstream from the accelerator output. Its periodicity was chosen to be $D_g = 2.54$ mm in order to obtain first-order SPR frequencies centered at 120 GHz when $\theta \simeq 0$. Thus, for bunches as long as 300 μm, the power reduction due to bunch length at frequencies as high as $\sim$160 GHz would not be more than 15%. To obtain high efficiency, an echelle-type geometry was used and the blaze angle was optimized to $\alpha = 30°$. The grating overall length was 50.8 mm (20 periods). A grating width of $W = 100$ mm was chosen to reduce possible finite-width effects when comparing to theory [2]. The grating thickness was 10 mm for mechanical strength. The finite thickness of the grating has a very small effect on the intensity of the radiation, as shown in [21], but the effect is negligible at the observation angles of interest in this experiment. The grating was installed on two stepper motor feedthroughs which were used to independently adjust the height of the beam from the front and back of the grating.

A 200 mm diameter by 12.7 mm thickness fused quartz vacuum window was located 150 mm from the center of the beam line, allowing a clear view of the grating at angles up to $\pm 18°$. The window transmission was cold tested at a frequency range of 90 to 140 GHz using an Agilent vector network analyzer. Based on this measurement the real part of the refractive index and the loss tangent were extracted and the window transmission as a function of the incident angles and frequency, $T_w(\theta, \phi, \omega)$, was calculated.

Measurements of the radiated power were made using microwave detector receivers located about 0.6 to 1 m away from the grating for far-field measurements. Receivers were built for each of two microwave bands. The first band, called W-band, uses standard components in WR10 waveguide and nominally covers the frequency band 75 to 110 GHz. The second band is D-band, uses WR6 waveguide components, and nominally covers the frequency band 110 to 170 GHz. In each band, the receiver consisted of a rectangular horn antenna and microwave detector for that band. The receiver was mounted on a pitch-yaw remote-controlled rotation stage to maximize the horn antenna directivity. For angles $\theta < 0°$ a WR10 receiver was used, and for angles $\theta > -5°$ a WR6 receiver was used, thus allowing a 5° overlap in covering the observation angles.

The detector power, P_d, is correlated to the SPR power density, S_n, by $P_d = S_n T_w A_e / r^2$, where $A_e = (\lambda^2/4\pi) G_r$ is the effective aperture of the horn antenna located at distance r from the grating, and G_r is the antenna maximum gain. To allow a direct comparison between experiment and theory, the measured power was normalized to units of W/sr by multiplying by the factor $r^2/T_w A_e$.

III. RESULTS

The transverse beam profile was measured by using the grating to intercept some portion of the beam before it reached the Faraday Cup. This interception data was used to evaluate the beam profile, yielding a FWHM of 1 mm. This number was used in the theoretical calculations for comparison with the experimental results.

In order to verify coherent radiation, the power was measured versus the beam current at observation angles of $\theta = 1°$ and 8°, both at $\phi_b = 0°$. The power was found to scale proportional to the square of the current, indicating coherent radiation, as expected at these frequencies.

The SPR resonance relationship, Eq. (1), was measured by using a tunable frequency meter. The frequency meter was placed between the antenna and the detector, and we scanned along θ while setting ϕ_b at 0°. Only discrete frequencies which correspond to the harmonics of the accelerator frequency were observed. These frequencies were present at the expected radiation directions, θ.

The radiation polarization was measured by rotating the horn antenna at $\theta = 1°$ and $\phi_b = 0°$. The radiation was polarized in the θ direction, as expected theoretically.

The coupling of the beam to the grating was measured by moving the grating with respect to the beam. The measured detector power in arbitrary units versus the beam height is shown in Fig. 2, where $\theta = 8°$ and $\phi_b = 7.6°$. The theoretical exponential decay for these parame-

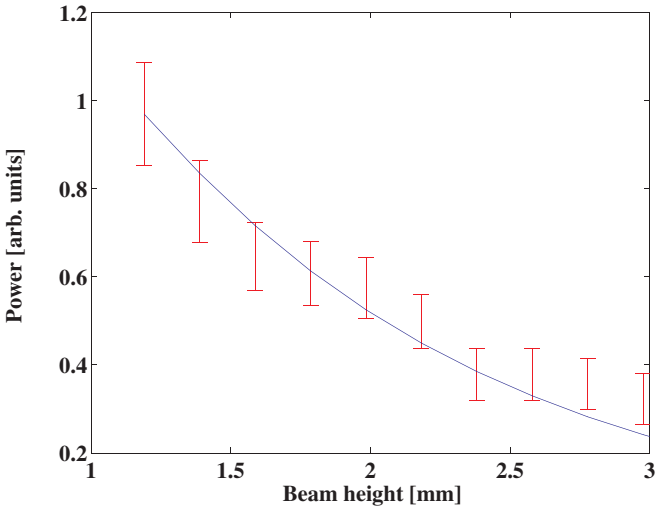

FIG. 2. (Color) Measured power vs beam height for $\theta = 8°$ and $\phi_b = 7.6°$. The solid lines describes the theoretical calculation for the parameters in Table I.

ters is shown by a solid line. Good agreement is shown between the experimental and theoretical results. Similar agreement was obtained for other sets of observation angles (not shown).

The SPR pattern was measured by scanning the antenna and detector along θ. The comparison, in units of W/sr, is shown in Figs. 3(a) and 3(b) for setting ϕ_b to 0° and 7.6°, respectively. In these figures the experimental results are shown by dots with error bars. The theoretical calculation by the EFIE model [2] and Eq. (3) is shown by the solid lines. Very good absolute-scale agreement was obtained between the experimental results and the EFIE calculations at all angles of observation.

In Figs. 3(a) and 3(b) each arrow indicates the frequency in which most of the power is emitted for the range of angles shown. This is further explained in Fig. 4 where the contents of the first-order radiated power density, calculated for $\phi_b = 0°$ by the EFIE model at the 6th, 7th, and 8th harmonics of the accelerator frequency, are shown by dotted, dashed, and dash-dotted lines, respectively. Their summation, shown by a solid line, agrees with the EFIE calculation in Fig. 3(a), where in Fig. 3(a) all relevant frequencies by Eq. (3) are included in the calculation.

Inspection of the calculated power spectrum revealed that the power peaking at angles $\theta = -8°, 1°$, and 8° is concentrated mostly at the 6th, 7th, and 8th harmonics of the accelerator frequency (102.84, 119.98, and 137.12 GHz), respectively. The angular width of each lobe is related to the grating periodicity and length and to the train frequency.

IV. DISCUSSION AND CONCLUSION

The purpose of this experiment was to test the accuracy of the finite grating length EFIE model. Frequency-locked

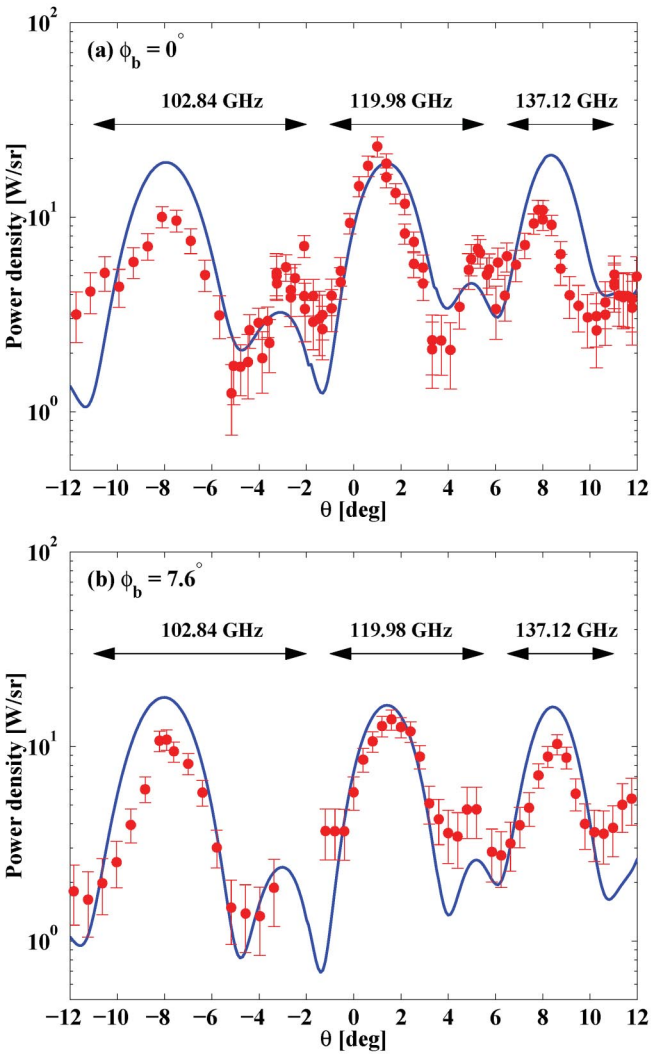

FIG. 3. (Color) Measured power density in W/sr (dots with error bars). The measurement is compared to the first-order radiated power density by the EFIE model (solid line). The power is plotted versus θ when $\phi_b = 0°$ (a) and $\phi_b = 7.6°$ (b). In these figures, each arrow spans over a range of angles in which the power is dominated by one discrete frequency (see Fig. 4).

SPR was generated by a train of bunches moving above the grating, and it was shown to be coherent at the millimeter wave range. Absolute-scale power measurements were obtained at a range of observation angles. The results were compared to the EFIE model which was modified for a train of bunches. We scanned the observation angles in the range of $-12° < \theta < 12°$ for $\phi_b = 0°$ and 7.6°. As seen in Figs. 3(a) and 3(b), the data reported agreed very well with the EFIE model.

It is noted that theories which assume a very large or an infinite number of grating periods, such as the image-charge [18] or van den Berg [15] model, respectively, could not be applied to calculate the power from a train of bunches. Such an assumption results in a very narrow, or even a δ function distribution of the radiated wavelength at

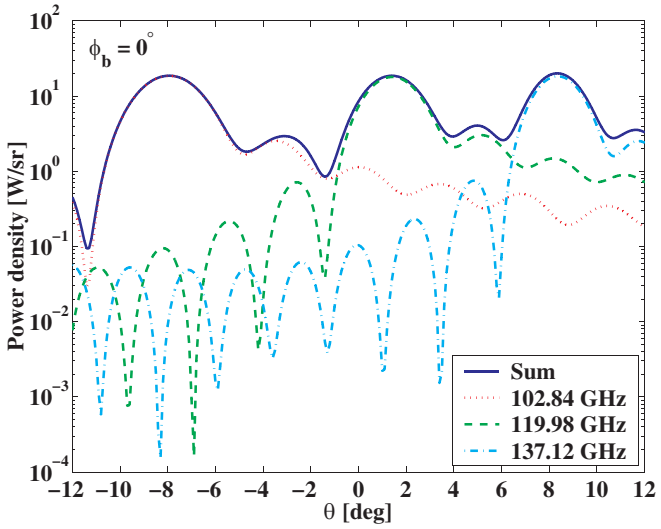

FIG. 4. (Color) First-order radiated power density calculated for $\phi_b = 0°$ by the EFIE model and Eq. (3) (solid line). This calculation was composed from the 6th (dotted line), 7th (dashed line), and 8th (dash-dotted line) harmonics of the accelerator frequency.

each observation angle. Since the SPR from a periodic train of bunches is locked to the train frequency in discrete harmonics [13], the radiation from an infinitely long grating would be observed only at discrete angles (θ_m, ϕ_m) fulfilling the SPR resonance relationship (1) at these discrete wavelengths

$$\lambda_m = \frac{D_g}{n}\left(\frac{1}{\beta} - \sin\theta_m \sin\phi_m\right) = \frac{2\pi c}{\omega_m}, \qquad (4)$$

where c is the speed of light and there is 1 degree of freedom in choosing the (θ_m, ϕ_m) pair.

In contrast, the finite grating length EFIE model allowed the SPR power generated by the train of bunches to be calculated over a continuous range of angles. As verified by the experimental results and demonstrated in Figs. 3 and 4, the power at the locked frequencies was radiated in angularly broadened directions due to the finite length of the grating. This experiment supports the EFIE model and demonstrates that finite-length calculation is necessary in order to accurately predict absolute power levels.

SPR can be used as a nondestructive bunch-length measurement for a single bunch or for the average bunch length in a train of bunches. The bunch length could be determined by either measuring the radiation pattern in arbitrary units and determining the cutoff angle or by measuring the radiation in absolute-scale units at a single observation angle, as suggested in [2]. Both methods require an accurate model to compare to. This work may also be important for SPR as a coherent radiation source [32,33], or for acceleration [34,35].

According to constraints from the EFIE model, we chose a wide enough grating in order to minimize possible finite-width errors for our operating parameters. It may be of interest to extend the model for finite-width gratings to support experiments in which the beam is of higher energy.

ACKNOWLEDGMENTS

The authors thank Ivan Mastovsky, Bill Mulligan, Jagadishwar Sirigiri, and Monica Blank. This research is supported by the U.S. Department of Energy, Division of High Energy Physics, Contract No. DE-FG02-91ER40648.

[1] S. J. Smith and E. M. Purcell, Phys. Rev. **92**, 1069 (1953).
[2] A. S. Kesar, Phys. Rev. ST Accel. Beams **8**, 072801 (2005).
[3] J. S. Nodvick and D. S. Saxon, Phys. Rev. **96**, 180 (1954).
[4] M. C. Lampel, Nucl. Instrum. Methods Phys. Res., Sect. A **385**, 19 (1997).
[5] D. C. Nguyen, Nucl. Instrum. Methods Phys. Res., Sect. A **393**, 514 (1997).
[6] S. E. Korbly, A. S. Kesar, R. J. Temkin, and J. H. Brownell (to be published);S. E. Korbly, A. S. Kesar, R. A. Marsh, and R. J. Temkin, in *Proceedings of the Particle and Accelerator Conference, Knoxville, TN, 2005* (IEEE, Piscataway, NJ, 1998).
[7] G. Doucas, M. F. Kimmitt, J. H. Brownell, S. R. Trotz, and J. E. Walsh, Nucl. Instrum. Methods Phys. Res., Sect. A **474**, 10 (2001).
[8] A. Doria, G. P. Gallerano, E. Giovenale, G. Messina, G. Doucas, M. F. Kimmitt, H. L. Andrews, and J. H. Brownell, Nucl. Instrum. Methods Phys. Res., Sect. A **483**, 263 (2002).
[9] G. Kube *et al.*, Phys. Rev. E **65**, 056501 (2002).
[10] K J. Woods, J. E. Walsh, R. E. Stoner, H. G. Kirk, and R. C. Fernow, Phys. Rev. Lett. **74**, 3808 (1995).
[11] K. Ishi, Y. Shibata, T. Takahashi, S. Hasebe, M. Ikezawa, K. Takami, T. Matsuyama, K. Kobayashi, and Y. Fujita, Phys. Rev. E **51**, R5212 (1995).
[12] Y. Shibata *et al.*, Phys. Rev. E **57**, 1061 (1998).
[13] S. E. Korbly, A. S. Kesar, J. R. Sirigiri, and R. J. Temkin, Phys. Rev. Lett. **94**, 054803 (2005).
[14] P. M. van den Berg, J. Opt. Soc. Am. **63**, 689 (1973).
[15] P. M. van den Berg, J. Opt. Soc. Am. **63**, 1588 (1973).
[16] O. Haeberlé, P. Rullhusen, J.-M. Salomé, and N. Maene, Phys. Rev. E **49**, 3340 (1994).
[17] J. Walsh, K. Woods, and S. Yeager, Nucl. Instrum. Methods Phys. Res., Sect. A **341**, 277 (1994).
[18] J. H. Brownell, J. Walsh, and G. Doucas, Phys. Rev. E **57**, 1075 (1998).
[19] S. R. Trotz, J. H. Brownell, J. E. Walsh, and G. Doucas, Phys. Rev. E **61**, 7057 (2000).
[20] J. H. Brownell and G. Doucas, Phys. Rev. ST Accel. Beams **8**, 091301 (2005).
[21] A. S. Kesar, M. Hess, S. E. Korbly, and R. J. Temkin, Phys. Rev. E **71**, 016501 (2005).
[22] A. Gover, P. Dvorkis, and U. Elisha, J. Opt. Soc. Am. B **1**, 723 (1984).
[23] J. E. Walsh, Nucl. Instrum. Methods Phys. Res., Sect. A **445**, 214 (2000).

[24] G. Doucas, M. F. Kimmitt, A. Doria, G. P. Gallerano, E. Giovenale, G. Messina, H. L. Andrews, and J. H. Brownell, Phys. Rev. ST Accel. Beams **5**, 072802 (2002).
[25] G. Doucas, M. F. Kimmitt, Th. Kormann, G. Korschinek, and C. Wallner, Int. J. Infrared Millim. Waves **24**, 829 (2003).
[26] J. Haimson, IEEE Trans. Nucl. Sci. **12**, 996 (1965).
[27] J. Haimson, B. Mecklenburg, G. Stowell, K. E. Kreischer, and I. Mastovsky, in *High Energy Density Microwaves*, edited by Robert M. Phillips, AIP Conf. Proc. No. 474, 137 (1999).
[28] J. Haimson and B. Mecklenburg, in *Proceedings of the 1995 Particle Accelerator Conference, Dallas, TX* (IEEE, Piscataway, NJ, 1995), pp. 755–757; Cat. No. 95CH35843.
[29] W. J. Mulligan, S. C. Chen, G. Bekefi, B. G. Danly, and R. J. Temkin, IEEE Trans. Electron Devices **38**, 817 (1991).
[30] J. Haimson, B. Mecklenburg, G. Stowell, and B. Ishii, in *Advanced Accelerator Concepts: Tenth Workshop*, edited by Christopher E. Clayton and Patrick Muggli, AIP Conf. Proc. No. 647 (AIP, New York, 2002), p. 810.
[31] J. Haimson, in *Advanced Accelerator Concepts: Eleventh Advanced Accelerator Concepts Workshop*, edited by Vitaly Yakimenko, AIP Conf. Proc. No. 737 (AIP, New York, 2004), p. 95.
[32] A. Halperin, A. Gover, and A. Yariv, Phys. Rev. A **50**, 3316 (1994).
[33] J. T. Donohue and J. Gardelle, Phys. Rev. ST Accel. Beams **8**, 060702 (2005).
[34] Y. Takeda and I. Matsui, Nucl. Instrum. Methods **62**, 306 (1968).
[35] K. Mizuno, S. Ono, and O. Shimoe, Nature (London) **253**, 184 (1975).